Detailed Vertebral Segmentation Using Part-Based Decomposition and Conditional Shape Models

Marco Pereañez, Karim Lekadir, Corné Hoogendoorn, Isaac Castro-Mateos and Alejandro Frangi

Abstract With the advances in minimal invasive surgical procedures, accurate and detailed extraction of the vertebral boundaries is required. In practice, this is a difficult challenge due to the highly complex geometry of the vertebrae, in particular at the processes. This paper presents a statistical modeling approach for detailed vertebral segmentation based on part decomposition and conditional models. To this end, a Vononoi decomposition approach is employed to ensure that each of the main subparts the vertebrae is identified in the subdivision. The obtained shape constraints are effectively relaxed, allowing for an improved encoding of the fine details and shape variability at all the regions of the vertebrae. Subsequently, in order to maintain the statistical coherence of the ensemble, conditional models are used to model the statistical inter-relationships between the different subparts. For shape reconstruction and segmentation, a robust model fitting procedure is introduced to exclude outlying inter-part relationships in the estimation of the shape parameters. The experimental results based on a database of 30 CT scans show significant improvement in accuracy with respect to the state-of-the-art and the potential of the proposed technique for detailed vertebral modeling.

M. Pereañez (✉)
Center for Computational Imaging and Simulation Technologies in Biomedicine (CISTIB), Universitat Pompeu Fabra, 08018 Barcelona, Spain
e-mail: marco.pereanez@upf.edu

K. Lekadir · C. Hoogendoorn
CISTIB, Universitat Pompeu Fabra, 08018 Barcelona, Spain
e-mail: karim.lekadir@upf.edu

C. Hoogendoorn
e-mail: corne.hoogendoorn@upf.edu

I. Castro-Mateos · A. Frangi
CISTIB, University of Sheffield, S1 3JD, Sheffield, UK
e-mail: isaac.casm@sheffield.ac.uk

A. Frangi
e-mail: a.frangi@sheffield.ac.uk

J. Yao et al. (eds.), *Recent Advances in Computational Methods and Clinical Applications for Spine Imaging*, Lecture Notes in Computational Vision and Biomechanics 20, DOI 10.1007/978-3-319-14148-0_9

1 Introduction

Automatic segmentation of the vertebrae is an important pre-requisite for a number of clinical applications, ranging from the assessment of spinal disorders to image-guided interventions. The latter one in particular, with the recent advances in minimal invasive surgical procedures, requires accurate and detailed extraction of the vertebral boundaries. However, this is challenging in practice due to the highly complex geometry of the vertebrae, in particular at the region of the processes. Figure 1 shows some examples of typical areas of high geometrical complexity and curvature in the lumbar vertebra L5.

Amongst existing techniques for vertebral image segmentation, statistical models of 3D shape [4] have been extensively used [2, 3, 5, 7, 8] due to their ability to build a shape prior from a representative training population. However, these methods consider at best a whole vertebra as the smallest unit for the construction of the point distribution models (PDMs). Due to the large variability of the vertebrae in particular at the processes and the generally small number of samples available for training, the obtained models are too constraining and not flexible enough to localize the fine details at areas of high curvatures.

In this paper, we present a new method for detailed modeling and segmentation of the vertebrae. The fundamental idea behind the proposed technique is to decompose each vertebra into a set of subparts based on their geometrical properties. By using a Vononoi [9] decomposition approach, we ensure that each of the main subparts of the vertebrae is well identified. With this approach, the shape constraints are effectively relaxed, allowing for an improved encoding of the fine details and shape variability at all the regions of the structures. Subsequently, in order to maintain the statistical coherence of the ensemble, conditional models are used to model the statistical inter-relationships between the different subparts. For shape reconstruction and segmentation, a robust model fitting procedure is introduced to exclude outlying

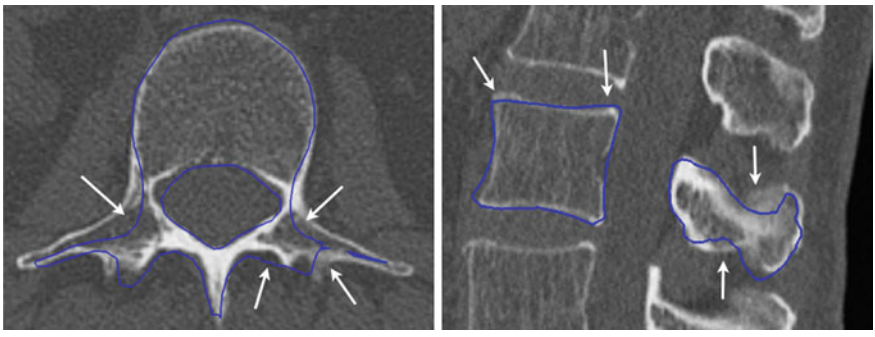

Fig. 1 Examples of segmentations (in *blue*) obtained with local PDMs, showing suboptimal fitting in areas of complex geometry and high curvature on the spine (Color figure online)

inter-part relationships in the estimation of the shape parameters. The proposed technique is validated with a total of 30 spinal CT scans.

2 Method

The proposed framework consists of three main stages. Firstly, in Sect. 2.1, a subdivision of each vertebra into a number of subparts is proposed based on an approximate Voronoi region decomposition. Subsequently, the conditional models describing the statistical inter-relationships between the subparts are presented in Sect. 2.2. Finally, a model fitting approach based on all pair wise conditional models is introduced in Sect. 2.3, with the aim to estimate the shape parameters for each subpart robustly.

2.1 Vertebral Decomposition

Let us denote $\mathbf{x} = (\mathbf{x}_1, \ldots, \mathbf{x}_n)^T$ the landmark-based shape representation of each vertebra, where n is the number of landmarks used to discretize the 3D shape. The aim of this section is to obtain a subdivision of $\mathbf{x}$ into K sub-components.

We do this in this paper by using a polygon clustering algorithm described in [9], which provides a compact subdivision of the shape based on the concept of a Voronoi diagram [1]. Furthermore, let us denote $V = (C_1, \ldots, C_m)^T$ the triangulation of the shape $\mathbf{x}$, where $C_i, i = 1, \ldots, m$, represents each face on the mesh, and E_j the set of edges between all adjacent triangles. Given the centroids c_i corresponding to each of the triangular triangles C_i, the algorithm computes an approximation of a centroidal Voronoi diagram (CVD). The energy term to minimize is:

$$F = \sum_{k=1}^{K} \left(\sum_{i \in R_k} w_i ||c_i - c_{R_k}||^2 \right), \tag{1}$$

where R_k is a subset of V (i.e. subpart of the shape), c_{R_k} is the center of the region, and w_i is the area of triangle C_i.

To minimize Eq. 1, we use an iterative approach over the subset of edges E_j between adjacent regions. The regions R_k are initialized as a single triangle that is randomly chosen amongst V. The remaining triangles are assigned to the *null* region R_0. We then iterate only over the edges that are between two regions R_k and R_l, or between any R_k and R_0. Then we assign one of the two triangles adjacent to the current edge to the region that minimizes Eq. 1. At some point, the region R_0 will become empty. The iterative algorithm will continue until no modification of the region assignments for the triangles lead to an improvement of the subdivision according to Eq. 1.

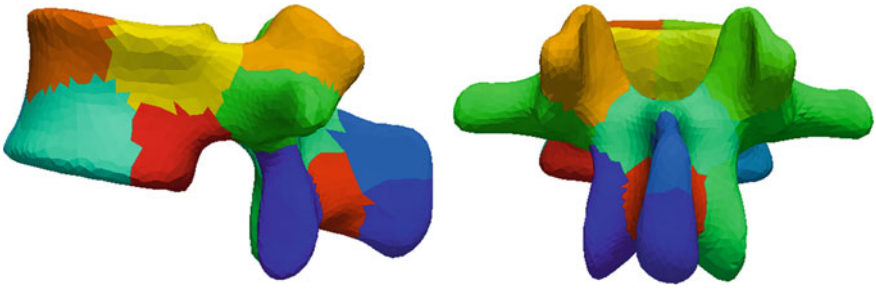

Fig. 2 The obtained Voronoi decomposition with 18 subparts

Given that the regions of highest complexity and curvature on the vertebra are the different vertebral processes, we chose the lowest number of clusters K such that points selected roughly at the distal region of every process (transverse, superior/inferior articular and spinous) are assigned to a different region after the subdivision.

Once the algorithm converges, all $C_i \in V$ will belong to a unique region R_i. However, the points that lie on the boundary edges between subparts will now belong to two adjacent regions. To resolve this ambiguity, we perform a last step where we go through the different regions sequentially and assign boundary points to the current region unless previously assigned.

Figure 2 shows the obtained subdivision with $K = 18$, where it can be seen that the main regions of high curvature now belong to a unique subpart.

2.2 Conditional Model Parametrization

In the previous section we obtained K subcomponents $\mathbf{x}_k$, $k = 1, \ldots, K$. The aim of this section is to describe the statistical modeling of the inter-part probability distributions, i.e. $P(\mathbf{x}_k|\mathbf{x}_l)$, where $k, l = 1, \ldots, K$ and $k \neq l$. More specifically, we would like to obtain new constraints for each part $\mathbf{x}_k$ based on its conditional relationship with $\mathbf{x}_l$, that is, a new mean and covariance in the space of the shape parameters $\mathbf{b}_k$. Let us denote μ_{kl} and Σ_{kl} the values that form the new conditional constraints. In this paper, we choose to model $P(\mathbf{x}_k, \mathbf{x}_l)$ using a normal probability distribution. Thus, the mean and the covariance estimates are calculated as:

$$\mu_{kl} = \Sigma_{kl} \Sigma_{ll}^{-1} \mathbf{b}_l \tag{2}$$

$$\Sigma_{kl} = \Sigma_{kk} - \Sigma_{kl} \Sigma_{ll}^{-1} \Sigma_{lk} \tag{3}$$

$\mathbf{b}_l$ in Eq. 2 is the parametric representation after eigendecomposition of the a given conditioning shape $\mathbf{S}_l$, and the covariance matrices in Eqs. 2 and 3 are obtained from the partitioned covariance matrix in Eq. 4:

$$\Sigma = \begin{bmatrix} \Sigma_{kk} & \Sigma_{kl} \\ \Sigma_{lk} & \Sigma_{ll} \end{bmatrix} \tag{4}$$

In Eqs. 2 and 3 $\Sigma_{kl}\Sigma_{ll}^{-1}$ are called the matrix regression coefficients of $\mathbf{b}_k$ on $\mathbf{b}_l$.

In order to compute the conditional mean μ and covariance matrix Σ, we need to compute the inverse of the covariance matrix of the predictor shape, however, as the dimensionality of the shapes is much larger than the number of training samples available, the covariance matrix becomes singular, and cannot be inverted. Also, the computational burden of computing inverse of matrices representing several thousands of points can become cumbersome. We address this issues by reducing the dimensionality of the problem using PCA before computation of the mean and covariance matrix as follows [6]:

given subshapes $\mathbf{x}_k$ and $\mathbf{x}_l$,

$$\mathbf{x}_k = \bar{\mathbf{x}}_k + \Phi_k \mathbf{b}_k \tag{5}$$

$$\mathbf{x}_l = \bar{\mathbf{x}}_l + \Phi_l \mathbf{b}_l, \tag{6}$$

their parametric representation is

$$\mathbf{b}_k = \Phi_k^T \mathbf{x}_k - \bar{\mathbf{x}}_k \tag{7}$$

$$\mathbf{b}_l = \Phi_l^T \mathbf{x}_l - \bar{\mathbf{x}}_l. \tag{8}$$

Then the cross-covariance matrix $\Sigma_{kl} = \mathbf{B}_k \mathbf{B}_l^T$ is the product of parametric shapes matrices $\mathbf{B}_k$ and $\mathbf{B}_l$. The self-covariance matrices Σ_{kk} and Σ_{ll} are the diagonal eigenvalue matrices Λ_k and Λ_l obtained by eigendecomposition of the individual subparts.

The proposed parametrization of the conditional model has two important benefits. Firstly, it decreases the over-constraining of the global model caused by the dimensionality disparity between the available samples and the natural variabilty of the shapes. Additionally, and as detailed in next section, the inter-part models can be used as a mechanism to find the optimal domain of valid subregions and exclude incorrect localized segmentations due to image inhomogeneities.

2.3 Robust Model Fitting

To maintain the coherence of the ensemble in spite of the decomposition, the estimation of the shape parameters must be carried out by considering all pairwise

conditional probabilities $P(\mathbf{x}_k|\mathbf{x}_l)$. This is challenging at the segmentation stage because all subparts are being optimized simultaneously, and therefore, there is a degree of uncertainty surrounding the values of the different $\mathbf{x}_l$ in $P(\mathbf{x}_k|\mathbf{x}_l)$. This could lead to inaccurate constraining and parameter estimation of $\mathbf{x}_k$ if some of the $\mathbf{x}_l, l = 1, \ldots, K, k \neq l$ are erroneous during the segmentation procedure. To address this problem, we use a median-based estimation approach to exclude potentially incorrect conditional relationships.

Firstly, we calculate the initial shape parameter $\mathbf{b}_k^0$ by projecting the boundary feature points (as obtained using normal search profile) onto the standard PDM of $\mathbf{x}_k$. Subsequently, we calculate $K-1$ shape parameters $\mathbf{b}_{kl}$ by considering the $K-1$ shape constraints formed by the conditional mean parameter μ_{kl} and its corresponding bounds λ_{kl} (derived from the eigenvalues of Σ_{kl}), i.e.,

$$\mathbf{b}_{kl} = \begin{cases} \mathbf{b}_k^0 & \text{if } |\mathbf{b}_k^0 - \mu_{kl}| \leq 3\sqrt{\lambda_{kl}} \\ \mu_{kl} + 3\sqrt{\lambda_{kl}} & \text{if } \mathbf{b}_k > \mu_{kl} + 3\sqrt{\lambda_{kl}} \\ \mu_{kl} - 3\sqrt{\lambda_{kl}} & \text{if } \mathbf{b}_k < \mu_{kl} - 3\sqrt{\lambda_{kl}} \end{cases} \tag{9}$$

Due to the fact that some subparts are inevitably erroneous during the image search due to imaging inhomogeneities, some of the $\mathbf{b}_{kl}$ values will be incorrect. To exclude these values and obtain a consensus robust estimation of the shape parameters, we use a median-based final estimation of $\mathbf{b}_{kl}$, i.e.,

$$\mathbf{b}_k^{final} = median(\mathbf{b}_{kl}). \tag{10}$$

3 Validation

We validate our method using 30 image volumes of the lumbar spine (L1-L5) from CT scans. The image datasets were collected at the National Center for Spinal Disorders (Budapest, Hungary). The images have an in-plane resolution of 0.6×0.6 mm and slice thickness of 0.62 mm. All images were manually segmented using open source software.

All segmentations were performed by preserving 98 % of the total variance, and allowing ± 3 standard deviations from the mean. All segmentations are performed following a leave-one-out scheme. Accuracy is measured as the RMS point to surface distance between the manual segmentations and the reconstructions. Furthermore, we compare the proposed approach against the results obtained with a standard ASM using single-vertebra PDMs.

Figure 3 shows the segmentation errors for all the 30 scans using both ASM methods. It is evident that the proposed technique outperforms the single model ASMs for nearly all cases (with the exception of case 24, with minor differences). The average improvement is of 16 % and in some cases the improvement is over

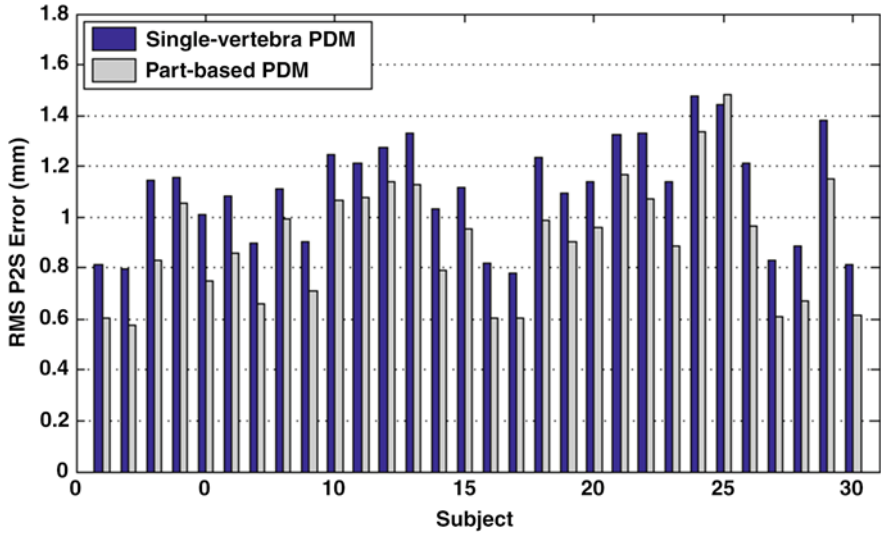

Fig. 3 Point to surface segmentation error comparison between the proposed method and a standard ASM single-vertebra PDM

Table 1 Image segmentation errors (mm) comparing the performance of our parts-based models (pb), and a single-vertebra PDM (sv). Errors are shown individually for each lumbar vertebra

Structure	L1		L2		L3		L4		L5	
	pb	sv	**pb**	sv	**pb**	sv	**pb**	sv	**pb**	sv
Mean	**0.81**	1.05	**0.82**	1.08	**0.84**	1.05	**0.88**	1.12	**1.06**	1.23
± Std	**0.13**	0.15	**0.15**	0.23	**0.17**	0.19	**0.20**	0.25	**0.24**	0.18

20 % due to the ability of the proposed technique to better encode the fine details of the vertebrae.

Table 1 summarizes the segmentation results for the proposed part-based technique (pb) and the single vertebra ASM (sv) for the different lumbar vertebrae (L1 to L5). It can be seen that the performance of the proposed technique is consistently better for the entire lumbar spine.

Finally, we show in Fig. 4 two illustrations of the error distribution for both the standard ASM and the proposed technique. It can be seen that the errors introduced locally by the use of a single vertebral model are corrected by the proposed parts-based approach. For both examples, the errors are consistently low in all regions of the vertebra.

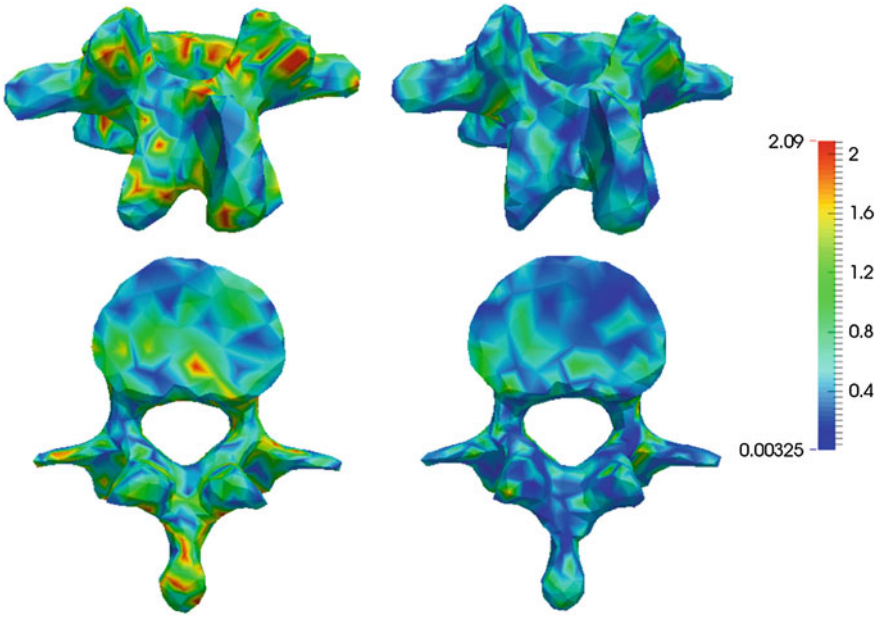

Fig. 4 Point to surface segmentation error comparison between the proposed method (*right top/bottom*), and a standard ASM single-vertebra PDM (*left top/bottom*)

4 Conclusions

In this paper, we presented a new part-based ASM approach for detailed segmentation of the lumbar vertebrae. The proposed technique addresses the difficulty to model the variability in the area of high complexity and curvature by decomposing the vertebrae into a set of subparts, which are subsequently linked using conditional shape models. A robust median-based estimation of the shape parameters of each subpart is used to minimize potential errors due to the presence of image inhomogeneities. The results indicate potential for more detailed localization of the fine details of the vertebrae. Future work include the study of the effect of the number of subparts on the models and segmentation properties.

References

1. Aurenhammer, F.: Voronoi diagrams: a survey of a fundamental geometric data structure. ACM Comput. Surv. (CSUR) **23**(3), 345–405 (1991)
2. Benameur, S., Mignotte, M., Parent, S., Labelle, H., Skalli, W., de Guise, J.: 3d/2d registration and segmentation of scoliotic vertebrae using statistical models. Comput. Med. Imaging Graph. **27**(5), 321–337 (2003)

3. de Bruijne, M., Nielsen, M.: Image segmentation by shape particle filtering. ICPR **3**, 722–725 (2004)
4. Cootes, T.F., Taylor, C.J., Cooper, D.H., Graham, J.: Active shape models—their training and application. Comput. Vis. Image Underst. **61**(1), 38–59 (1995). doi:10.1006/cviu.1995.1004
5. Kadoury, S., Labelle, H., Paragios, N.: Spine segmentation in medical images using manifold embeddings and higher-order mrfs. Med. Imaging, IEEE Trans. **32**(7), 1227–1238 (2013)
6. Metz, C., Baka, N., Kirisli, H., Schaap, M., van Walsum, T., Klein, S., Neefjes, L., Mollet, N., Lelieveldt, B., de Bruijne, M., et al.: Conditional shape models for cardiac motion estimation. In: Medical Image Computing and Computer-Assisted Intervention-MICCAI 2010, pp. 452–459. Springer (2010)
7. Rasoulian, A., Rohling, R., Abolmaesumi, P.: Lumbar spine segmentation using a statistical multi-vertebrae anatomical shape+pose model. Med. Imaging IEEE Trans. **32**(10), 1890–1900 (2013). doi:10.1109/TMI.2013.2268424
8. Roberts, M.G., Cootes, T.F., Adams, J.E.: Linking sequences of active appearance sub-models via constraints: An application in automated vertebral morphometry. In: BMVC, pp. 1–10 (2003)
9. Valette, S., Chassery, J.M.: Approximated centroidal Voronoi diagrams for uniform polygonal mesh coarsening **2**4(3), 381–389 (2004). doi:10.1111/j.1467-8659.2004.00769.x